The College of Engineering
University of Wisconsin-Madison

Wisconsin Electric Machines and Power Electronics Consortium

RESEARCH REPORT
89-8

Performance Testing of a High Frequency Link Converter for Space Station Power Distribution System

S.K. Sul, I. Alan, T.A. Lipo
University of Wisconsin
Dept. of Electrical & Computer Engineering
1415 Johnson Drive
Madison, WI 53706

WEMPEC

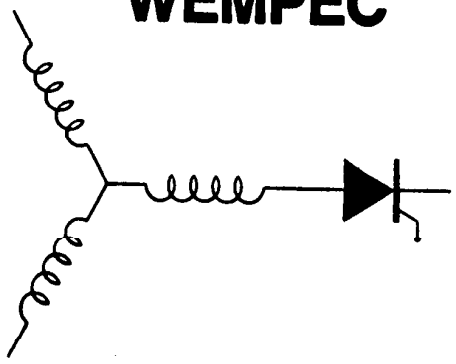

Department of Electrical and Computer Engineering
1415 Johnson Drive
Madison, Wisconsin 53706

899362

Performance Testing of a High Frequency Link Converter for Space Station Power Distribution System

S.K. Sul, I. Alan and T.A. Lipo
Department of Electrical and Computer Engineering
1415 Johnson Drive
University of Wisconsin
Madison WI 53706

ABSTRACT The testing of a brassboard version of a 20 KHz high frequency ac voltage link prototype converter manufactured by General Dynamics for space station application is presented. The General Dynamics Converter (GDC) is based on the three phase six pulse bridge concept developed at the University of Wisconsin. The testing includes details of the operation of the converter when driving an induction machine source/load. By adapting a Field Orientation Controller (FOC) to the GDC, four quadrant operation of the induction machine from the converter has been achieved. Circuit modifications carried out to improve the performance of the converter are described. The performance of two 400 Hz induction machines powered by the converter with simple V/f regulation mode is reported. Finally, the testing and the performance of the GDC utilizing a FOC, which provides the capability of rapid torque changes, speed reversal and four quadrant operation is presented.

INTRODUCTION

The traditional and most widely used type of static power frequency changer is the Pulse Width Modulated (PWM) inverter. PWM inverters can be characterized by the use of a dc voltage link for an intermediate step in the conversion of fixed frequency power to variable frequency power. The intermediate step allows for decoupling of the input and output by establishing a reservoir of reactive energy. Recent advances in power conversion has opened a way for systems to utilize a high frequency ac link as an intermediate step. In this case the intermediate voltage bus is established by a parallel resonant LC tank so that the bus voltage alternates at 20 KHz. The features of the two different types of links can be summarized as follows.

DC LINK

- Ideal for temporary energy storage and can be easily accomplished at relatively low cost,
- Hard switching of power devices generates a high level of losses and device stresses and therefore necessitates large heat sinks and limits the switching frequency to a few kHz,
- Lower switching frequency (typical medium size 10-50 kW PWM inverter, at best 5 kHz) results in poorer system response, reduced gains for high power densities and increased output frequencies, and troublesome audible and electrical noise,
- Bi-directional power flow is only possible with considerable additional expense.

AC LINK

- Relatively reduced energy storage capacity can be achieved at the expense of recognizing a moderate variation of link voltage,
- Soft switching of power devices reduces device stresses and switching losses and therefore does not require larger heat sink sizes and enables switching at twice the frequency of the resonant tank circuit (typically 40 kHz),
- Faster switching frequency results in dramatic gains in system response, increased power densities, increased output frequencies, and reduced audible and electrical noise,
- Allows flexibility for stepping the link voltage up/down through transformers for individual sources/loads which also assists in electrical isolation of the link from sources/loads,
- Has bi-directional power flow capability at the expense of having twice as many devices compared to the dc link converter, but anticipated cost effective bi-directional devices is expected to overcome this problem.

Since these new converters have the benefit of lower power dissipation, light weight, and low noise, the application of this technology is promising, particularly in an isolated system such as the proposed NASA space station. In this case the high frequency link can be utilized as the distribution link making possible single or three phase variable frequency, variable voltage power as well as adjustable voltage dc power readily available throughout the space station [1]. The most recent implementation of these high frequency link concepts is a brassboard constructed by General Dynamics/Convair of San Diego using concepts developed at the University of Wisconsin (UW) [2,3]. In this paper, the test results obtained from the General Dynamics Converter (GDC) configured at UW as a variable frequency and variable voltage (or current) ac motor controller are presented [4-6].

OVERALL SYSTEM DESCRIPTION

The overall system investigated in this paper is shown in Fig. 1 [2]. In this system a 20 kHz high frequency ac link is established by a well known classical inverter, the so called Parallel Series Output Resonant (POSR) inverter [7]. The 20 kHz bus thus established is used as the input source by the GDC. The principle of operation of this converter is described in Ref. [3]. To be able to simulate the real ac link power distribution system and match the operating voltage requirement of each individual converter, transformers at the output of the POSR and at the input of the GDC are used. Each of these converters have their own resonant tank circuits which in turn serves to establish and maintain the 20 kHz ac link and also functions as a temporary energy storage element in much the same manner as the dc link capacitor of a PWM inverter. The tank circuit is tied to the GDC converter by means of an isolation transformer. The switches in the interface converter have bi-directional current flow and voltage blocking capability. As a load for the interface converter two 400 Hz induction machines were used. The specifications for these induction machines are given in Table 1.

Another dc machine is used as a load (or prime mover) for the induction machines during motor (or generator) operation. The converter has the capability of being driven in either a voltage or current regulation mode through a computer terminal or by means of a current regulation mode using a field oriented controller (FOC). As it can be seen from the figure, the FOC has

CH2781-3/89/0000-0617 $1.00 © 1989 IEEE

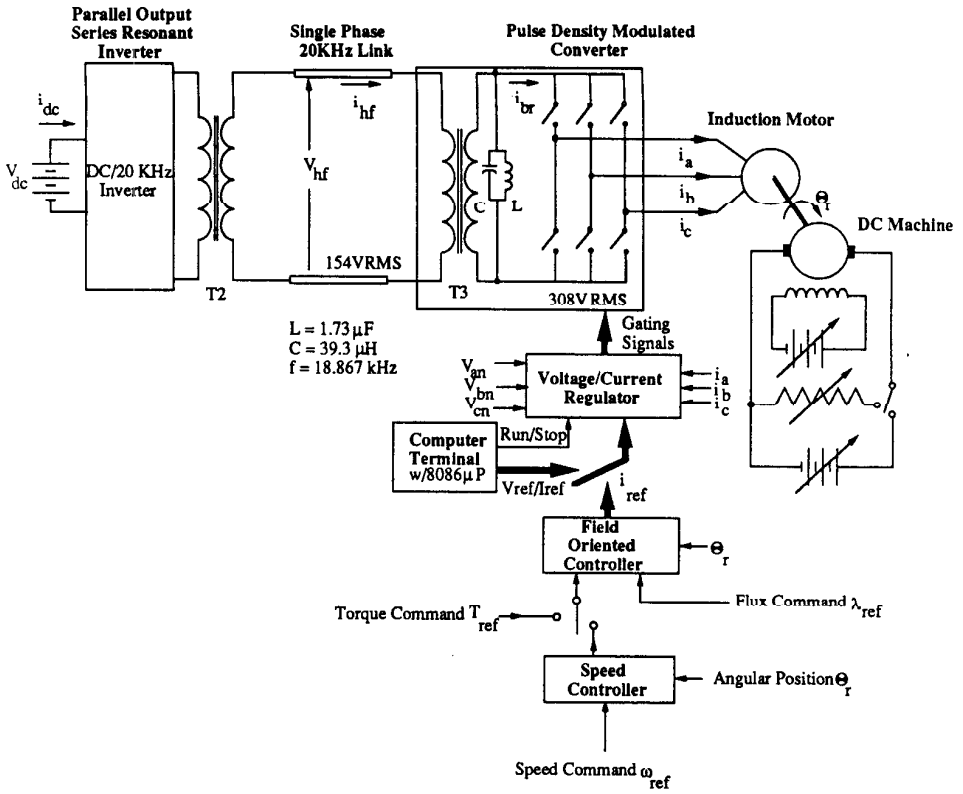

Fig. 1 Overall System Layout Utilizing POSR Converter, Step Up and Step Down Transformers, Resonant Link High Frequency Link Converter and Induction Machine Load.

its own control choices, one of which is a torque control mode, the other being a speed control mode. Both of these modes generate a torque command depending on the desired reference quantities and this torque command along with the flux command generates 3 phase ac current references for the converter-induction machine pair.

CIRCUIT MODIFICATIONS

Before the adaptation to a four quadrant motor controller, the GDC itself has undergone several modifications. In particular, the location of the resonant tank circuit was changed from the primary side to the secondary side of the input transformer of the GDC as indicated in Fig. 1. This change was made because the link current into the converter changes very rapidly with the switching of the converter. The new location of the tank circuit reduces the spikes and improves the link voltage switched by the converter.

After relocating the tank circuit, the timing circuit was also modified to obtain the exact zero crossing point in order to reduce the switching losses of the converter. Also a dead time was added to prevent a possible shoot through of the link due to the simultaneous turn on of the top and bottom switches. Modifications gave rise to switchings at almost exact zero crossings of the link.

Although the current sensors in the original circuit were wide band current transformers they were incapable of measuring current at dc or low frequency. Therefore, all of the current sensors were changed to Hall Sensors which have a frequency range from dc to 100 kHz. Also, problems were encountered with system grounds. To measure the output voltages without a common ground, a new circuit, developed in the earlier work for NASA [3], was installed. This new circuit synthesizes the output voltages of the converter from the link voltage and corresponding gating signals.

Parameters	1 HP Machine	2 HP Machine
Rated Voltage	208 V	208 V
Rated Frequency	400 Hz	400 Hz
Number of Poles	12	8
Rated Torque	16.98 lb-in	22.14 lb-in
Rated Current	4.5 Amp	10 Amp
Rated Speed	3716 RPM	5684 RPM
Efficiency at Rated Torque and Speed	75 %	80.95 %
Power Factor at Rated Torque and Speed	0.566	0.636

Table 1 Specifications of 1 and 2 HP Induction Machines.

Finally, in the original design, the over-current protection was handled by changing the gating logic from normal operation to current suppression operation . However, such a protection scheme could not handle the possibility of power semiconductor failure. To prevent this problem the control was modified so that all of the gating signals were removed whenever an over-current situation occurs. It should be mentioned, however, that this type of protection also involves a trade-off. If all the gating signals are removed in the presence of over-current, the current of the induction machine has no path to flow. Therefore, the energy stored in the inductance of the machine can impose a voltage spike to all switches which may result in a failure of one or more switches. In the case of a machine of a few horsepower, this problem can be easily solved by incorporating surge absorbers between the output phases. However, for high power applications over 10 kW, surge absorbers do not help the problem. A final solution to the problem will require further research.

STEADY STATE OPERATION OF THE GDC

In this section, the steady state operating characteristics of the high frequency link converter are presented. A 2 HP, 400 Hz induction machine was used operating in the voltage regulation mode (constant volts/Hz) from 200-400 Hz and two thirds of the rated load torque. The overall system block diagram for these tests is shown in Fig. 1. In particular, to simulate the real distribution line and to match the voltage ratings, 20 kHz transformers are used on both sides of the link.

20 kHz POSR Inverter:

The output voltage and input current waveforms of the 20 kHz Parallel Output Series Resonant (POSR) inverter are shown in Fig. 2. It can be noted that the ouput voltage has some fluctuation because of the power transfer between the POSR inverter and the GDC. The current waveform has a large peak to peak value but a small average value, which indicates that the converter must handle large reactive power even during conditions of small active power. To obtain a better link voltage regulation, the peak to peak current should be large. This is one of the well known disadvantages of the POSR inverter.

20 kHz AC Link:

The link voltage and link current waveforms, v_{hf} and i_{hf} are shown in Figs. 3 and 4. Even though the resonant link voltage is almost purely sinusoidal, the link current waveform shows some harmonics. However, its fundamental component

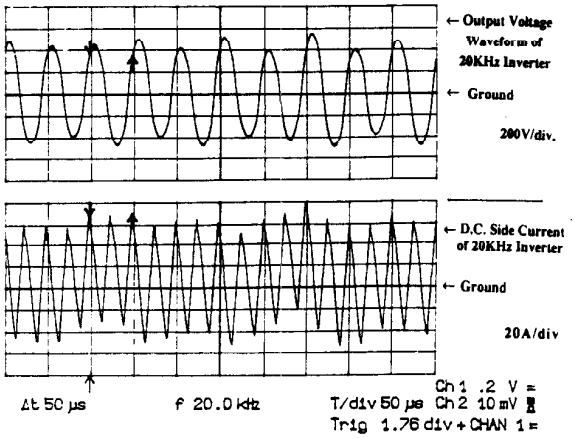

Fig. 2 Output Voltage and Input Current Waveforms of the 20 kHz Parallel Output Series Resonant Converter.

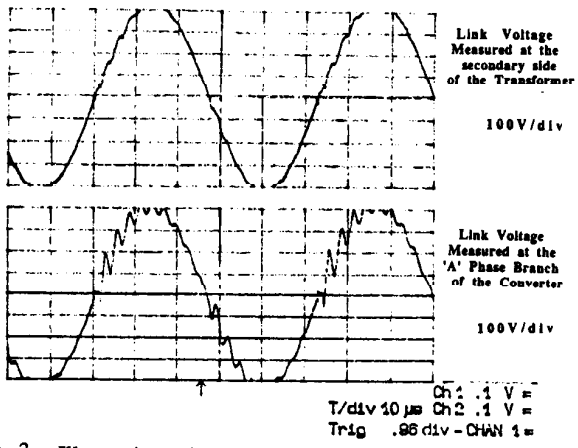

Fig. 3 Illustrating Effects of Stray Inductance. Upper Trace Shows Voltage Across Resonant Tank. Lower Trace Shows Voltage Across Converter Branch Corresponding to Phase *a*.

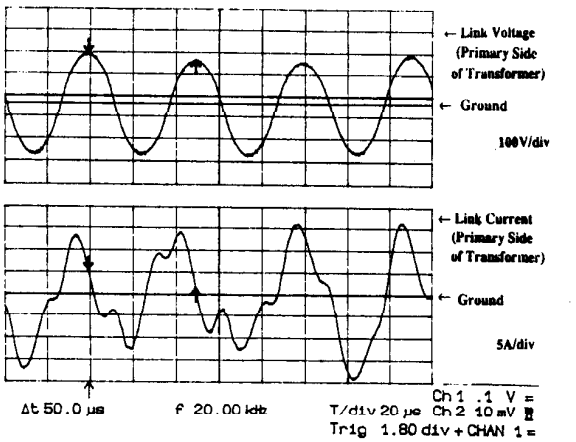

Fig. 4 Link Voltage and Link Current of 20 kHz Resonant Tank.

is clearly 20 kHz.

Interface Converter (GDC):

The voltage waveform across the GDC converter, measured at a point farthest from the resonant link capacitor in the physical circuit is shown in Fig. 5. Also shown is and the link current i_{br} which is identified in Fig. 1. Because of the resonance between the stray inductance and the snubber capacitors, the current waveform reveals very high frequency oscillations and a peak value which is considerably more than the average value.

The voltage waveforms across Q1 and Q4 are shown in Fig. 6. The waveforms clearly reveal complementary operation of two bi-directional switches and also zero voltage switching.

Induction Machine:

The line to line voltage and line current waveforms of the induction machine are shown in Fig. 7, where operating conditions are different from the previous waveforms. In this case, a 1 Hp, 400 Hz machine is operating at 300 Hz. To take a close look at the output voltage and the link current waveforms a magnified view of Fig. 7 is given in Fig. 8, where it is clearly shown that the line to line voltage is composed of many half cycle pulses of the resonant link voltage. The frequency

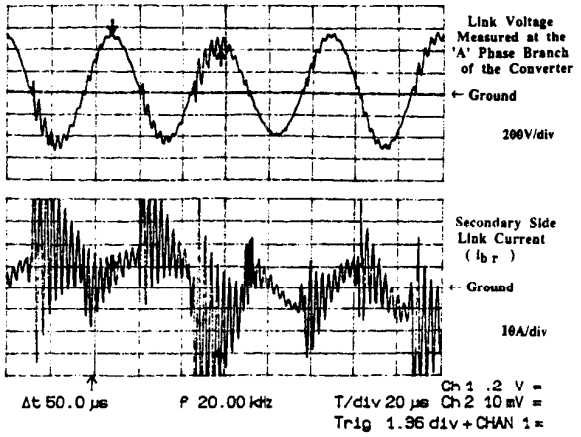

Fig. 5 Tank Voltage v_{br} Measured Near Position of Remotest Output Phase and Current i_{br} of High Frequency Link Converter (GDC).

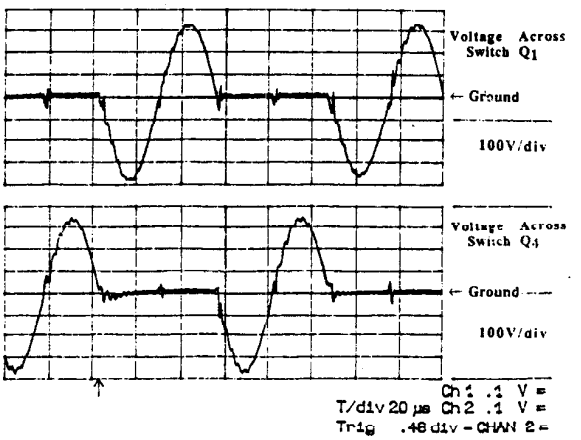

Fig. 6 Voltage Waveforms Across Q1 and Q4 Illustrating Zero Voltage Switching Capability.

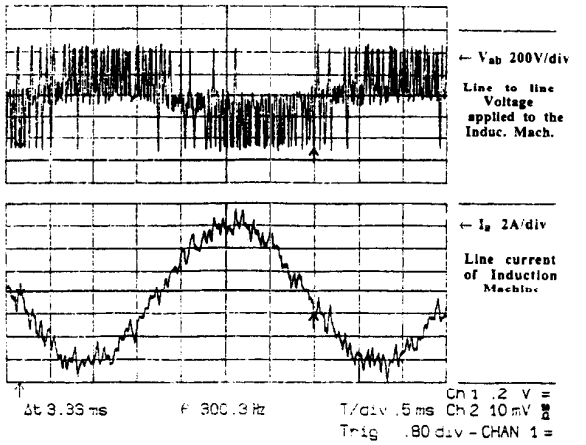

Fig. 7 Line to Line Voltage and Line Current of Induction Machine Load Operating at Rated Current.

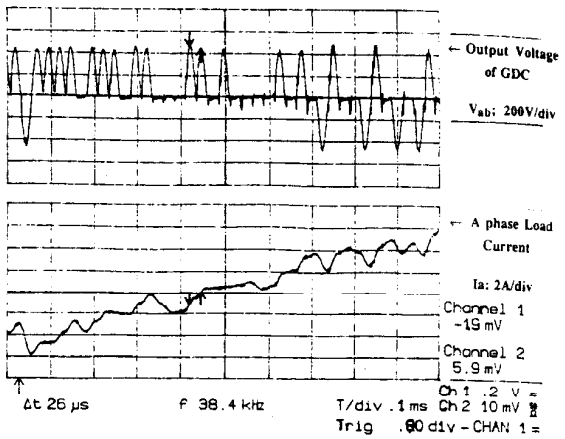

Fig. 8 Magnified View of Fig. 7.

spectrums of the output voltage and output current are given in Figs. 9 and 10. The spectrum of the voltage in Fig. 9 shows a large peak at the fundamental frequency and some harmonics after 2 kHz. In the frequency region from dc to 2 kHz, which is the most important frequency spectrum region, there are virtually no harmonics evident. The spectrum of the current waveform is quite different from that of the voltage waveform. Because of the inductance of the machine, the current due to the high frequency harmonic voltages was suppressed. In Fig. 10, there is no noticeable harmonics until 3.5 kHz.

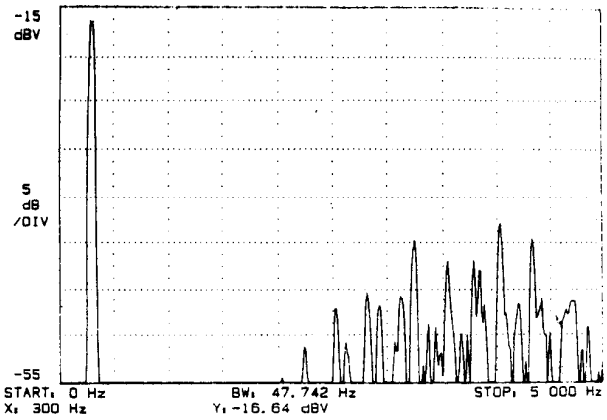

Fig. 9 Frequency Spectrum of Output Voltage V_{ab} over the Range 0 to 5 kHz.

PERFORMANCE OF AN INDUCTION MACHINE OPERATING FROM THE HIGH FREQUENCY LINK CONVERTER

In this section, the steady state performance of several induction machines driven by the GDC are reported. In particular, detailed steady state measurements were taken for a 2 Hp as well as a 1 HP, 400 Hz induction machine both in the motoring and generating mode of operation. The voltage regulation mode of the GDC was used to obtain a steady state operating point. Because of the pole number and the maximum

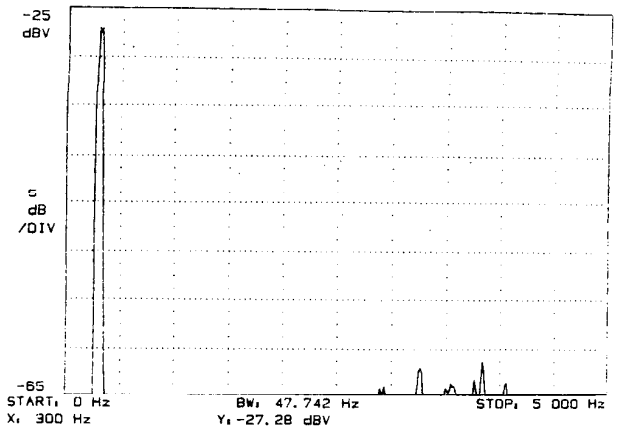

Fig. 10 Frequency Spectrum of *a* Phase Motor Current over the Range 0 to 5 kHz.

speed limitation of the DC machine, the 2 HP machine was tested at 100 Hz and 200 Hz, and the 1 HP machine at 200 Hz and 300 Hz. Since the efficiency is the most important performance parameter, it was carefully measured. The power factor was also measured throughout the test. For the purpose of measurement, two true rms power meters, which can also measure voltage and current were used. Also, to obtain some information about the fundamental voltage and current waveforms, a spectrum analyzer was utilized. The power meters used were Clark-Hess 259 Models which have a frequency response up to 100 kHz. The spectrum analyzer utilized was the HP 3651A Model. The efficiency obtained from the test was compared to the one obtained from computer simulation, where the harmonic losses and machine parameter variation with V/f change and frequency change were neglected. Hence, the efficiency obtained from computer simulation is substantially higher than the actual efficiency. It reflects the best possible efficiency since it assumes a sinusoidal input for the machine and neglects stray losses and iron losses.

For the 2 Hp machine, the computed and measured efficiency vs. torque curves are given in Fig. 11. In this figure, the best efficiency of the test result at 200 Hz operation is around 60% at 0.6 of the rated torque. The efficiency at 100 Hz is 40%. The large differences in the efficiency curves at different operating frequencies are mainly because of the large difference

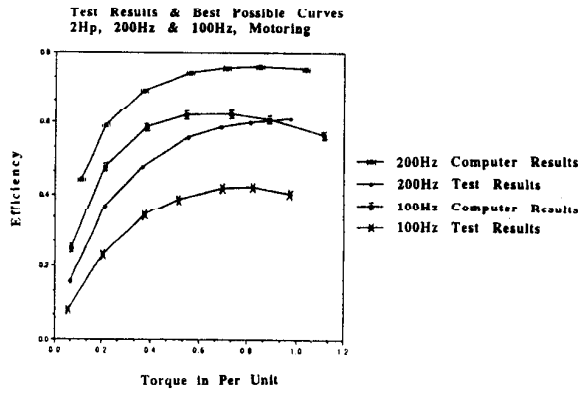

Fig. 11 Efficiency vs. Torque Curves for 2 HP Machine Operating at 100 and 200 Hz.

in power output between the two speeds. The differences between the computer simulation and the test results are due to the harmonic losses as well as the stray and iron losses. Usually the harmonic losses do not change proportionally to the torque, but remain nearly constant. It can be noted that the efficiency degrades rapidly with operating frequency as normally occurs in variable speed drives. In this particular test, the V/f ratio was set to its rated value.

The efficiency change with the variation of the V/f ratio is shown in Figs. 12 and 13. The variation of the V/f ratio suggests the benefits of a variation of the flux of the machine. There has recently been considerable research about efficiency improvement by changing the flux of the induction machine [8-12]. In Fig. 12 the efficiency vs. torque curves with the air gap flux as a parameter are shown. For the light load torque operation, the efficiency under reduced flux operation is higher than that for rated flux operation. However, for heavy load torque operation, the situation is reversed. This type of phenomenon is in agreement with recent research in the above references. This result suggests that for light loads the efficiency can be improved by decreasing the iron loss, but for heavy loads efficiency cannot be improved with reduced flux operation since the excessive copper losses needed to compensate reduced flux for a given load torque is greater than the iron loss saved by the reduced flux.

In Fig. 13, the efficiency change is more clearly shown with the variation of V/f ratio. It is clear that there is always an

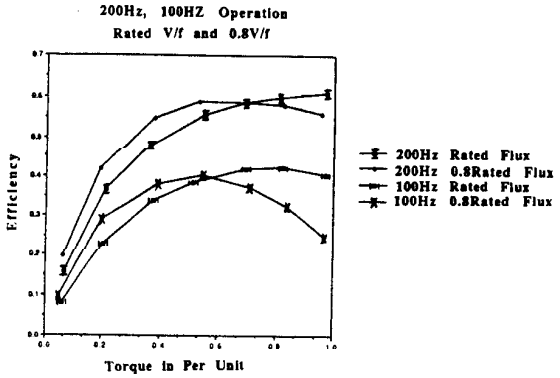

Fig. 12 Efficiency vs. Torque Curves for Two Values of Air Gap Flux.

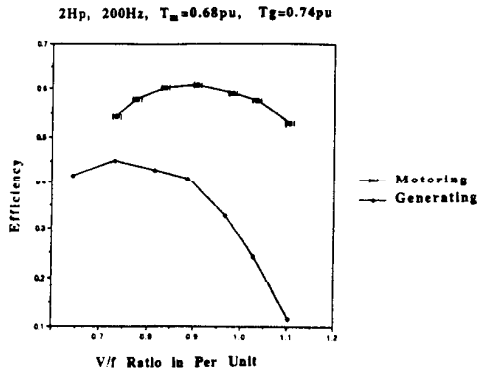

Fig. 13 Efficiency vs. Volts/Hertz Ratio for 2 HP Induction Machine.

optimal flux level which gives the best efficiency for a given mechanical torque. This figure shows that the efficiency of the generator operation is considerably worse than that of the motoring operation since for the same amount of mechanical power, the electrical power is greater than the mechanical power in motoring operation while it is smaller in generating operation. The curves between the power factor and the V/f ratio are shown in Fig. 14, where there are two kinds of power factors. The fundamental power factor, which is also called as displacement factor, has almost linear dependency on the V/f ratio, which can be explained by the change of the excitation current. The true power factor, including all harmonics, has a very small dependency on the V/f ratio. This fact can be explained as due to the high harmonics of the voltage waveforms since the rms voltage barely changes with the change of fundamental voltage. The slip frequency versus torque curves shown in Fig. 15, reveals the typical induction machine characteristics.

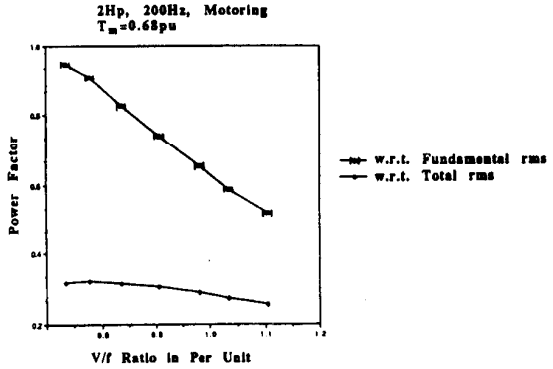

Fig. 14 Power Factor vs. Volts/Hertz Ratio for 2 HP Induction Machine.

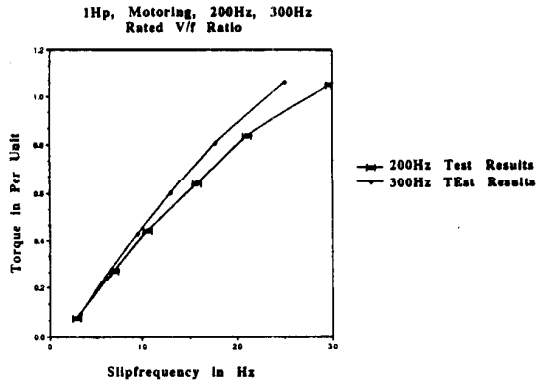

Fig. 15 Slip Frequency vs. Torque for 1 HP Induction Motor Operating at 200 and 300 Hz.

DYNAMIC PERFORMANCE OF THE INDUCTION MACHINE

In this section, the dynamic performance of an induction machine driven by the GDC and controlled by the current regulated Field Orientation Controller (FOC) is demonstrated. The 2 Hp induction machine is used and its speed was regulated either at the clockwise (CW) or counter clockwise (CCW) direction. A maximum speed of 2,700 rpm was selected throughout the test.

Speed Reversal:

The motor response during the speed reversal is shown in Figs. 16-18. In Fig. 16 the response of the speed and the torque command are shown. In particular, the machine is initially running CW at 2,700 rpm. When the reference polarity is suddenly changed, the machine decelerates rapidly and settles down in a CCW direction at 2,700 rpm. During this transient, the torque command is maintained at its negative maximum value to generate the full deceleration torque. In the steady state full speed condition, the torque command is only a small value to meet the friction torque. The induction machine was coupled with a DC machine, a torque sensor, and a speed encoder resulting in an appreciable system inertia. The entire system speed is changed from CW at 2,700 rpm to CCW at 2,700 rpm within 2 seconds. In this transient, the positive speed-negative torque and the negative speed-negative torque operations of the induction machine that cover two quadrants of the speed and torque plane are shown. A symmetrical result was obtained when the speed was changed in the reverse direction. The responses of the A phase load current during the speed reversal is shown in expanded form in Fig. 17. In this figure, excellent regulation of the current at dc or at very low frequency is clearly demonstrated. Also, the phase change of the A phase current during the reversal of speed can be easily observed. The A phase

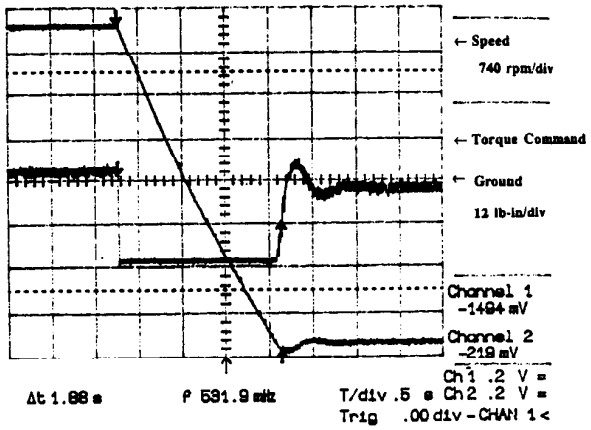

Fig. 16 Torque Command and Measured Speed During Speed Reversal (CW → CCW).

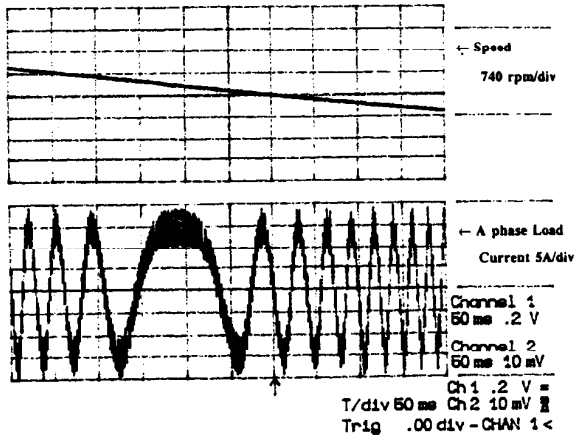

Fig. 17 Magnified View of Speed and *a* Phase Current During Speed Reversal.

current changes its phase not at zero speed but at about 400 rpm because of the effect of the slip frequency.

Load Torque Transients:

The response of the speed regulation for a load torque transient is shown in Fig. 18. In particular, the induction machine is spinning at 2,700 rpm without any load torque and the speed is constant. The speed is observed with ac coupling to remove the dc component and to determine the deviation of the speed in an accurate manner. The torque command supports only the friction load of the system. When two thirds of rated torque is suddenly applied as a load torque, the machine speed dips and the torque command increases to accommodate the increased load torque. After overshooting, the torque and the speed rapidly settles down. During this transient, the speed deviation is only 60 rpm. Almost symmetrical results were obtain for a sudden unloading of the machine. Since only a nominal effort was made in setting controller gains this speed regulation response could be even further improved by better tuning of the gains of the speed regulator.

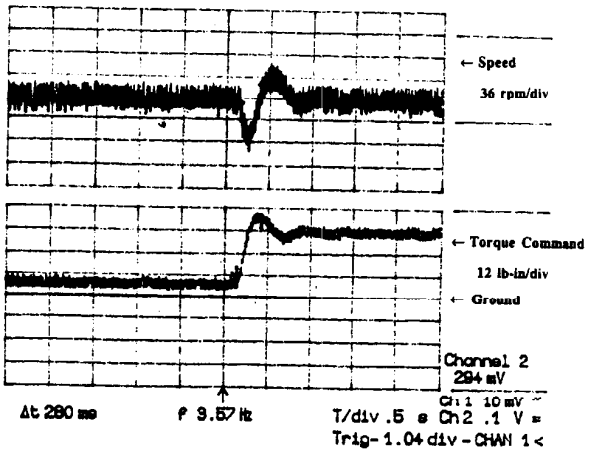

Fig. 18 Torque Command and Measured Speed During Application of a Sudden Load of 2/3 Rated Torque.

CONCLUSION

This report has summarized extensive tests carried out at the University of Wisconsin on a high frequency link converter constructed by General Dynamics/Convair. After some modification of the power and control circuitry and addition of a closed loop torque and speed controller, the converter has been shown to operate in a completely satisfactory fashion in all four possible quadrants of operation on the speed torque plane.

ACKNOWLEDGEMENTS

This work was sponsored by NASA Lewis Research Center, Cleveland OH under contract NAG 3-786. The authors wish to particularly thank Mr. Dave Peterson for making the POSR converter available for our use and to Mr. Ken Schreiner for help in making the equipment operational at the University of Wisconsin.

REFERENCES

1. I.G. Hansen, *Description of a 20 Kilohertz Power Distribution System*, 21st Intersociety Energy Conversion Engineering Conference (IECEC), San Diego, CA August 25-29, 1986..

2. K. Schreiner, *AC Bi-Directional Motor Drive Operation and Service Manual*, NASA Contract Report NASA CR-180866, General Dynamics-Space Systems Division, 1988.

3. P.K. Sood and T.A. Lipo, *Power Conversion Distribution System Using a Resonant High Frequency AC Link*, Conf. Rec. of IEEE IAS Annual Meeting, Oct. 1986, pp.

4. T.A. Lipo and P. Sood, *Study of the Generator/Motor Operation of Induction Machines in a High Frequency Link Space Power System*, NASA Report, Contract No. NAG3-631, Sept. 1986.

5. S.K. Sul and T.A. Lipo, *Design and Performance of a High Frequency Link Induction Motor Drive Operating at Unity Power Factor*, Conf. Record of IEEE IAS Annual Meeting, 1988, pp. 308-313.

6. S.K. Sul and T.A. Lipo, *Field Oriented Control of an Induction Machine in a High Frequency Link Power System*, Conf. Rec. of IEEE Power Electronics Specialists' Conference, Kyoto Japan, April 1988, pp. 1084-1090.

7. N. Mapham, *An SCR Inverter with Good Regulatioin and Sine Wave Output*, IEEE Trans. on Ind. & Gen. Appl., vol. IGA-3, pp. 176-187, Mar/Apr. 1967.

8. F.J. Nola, *Power Factor Controller - An Energy Saver*, in Conf. Rec. 1980 Annual Meeting IEEE Ind. Appl. Soc., pp. 194-198.

9. H.G. Kim, S.K. Sul, and M.H. Park, *Optimal Efficiency Drive of a Current Source Inverter Fed Induction Motor by Flux Control*, IEEE Trans. Ind.Appl. Vol. IA-20, No.6, pp. 1453-1459, Nov./Dec., 1984.

10. D. S. Kirschen, *Optimal Efficiency Control of Induction Machines*, Ph.D Thesis, Univ. of Wisconsin-Madison, 1985.

11. D. Kirschen, D. W. Novotny and T. A. Lipo, *On-Line Efficiency Optimization of a Variable Frequency Induction Motor Drive*, IEEE Trans. on Industry Applications, vol. IA-21, May/June 1985, pp. 610-616.

12. S.K. Sul, and M.H. Park, *A Novel Technique for Optimal Efficiency Control of a Current-Source Inverter-Fed Induction Motor*, IEEE Trans. Power Elec. Vol.3 No.2, pp. 192-199, 1988.